International Journal of Applied Pharmaceutics

ISSN- 0975-7058 Vol 17, Issue 1, 2025

Original Article

FORMULATION DEVELOPMENT AND PHARMACOKINETIC STUDIES OF NIRMATRELVIR LOADED SOLID LIPID NANOPARTICLES USING BOX-BEHNKEN DESIGN

REKHA M., SANGEETHA S.*

Department of Pharmaceutics, SRM College of Pharmacy, SRMIST, Kattankulathur, Chennai, Tamil Nadu, India
***Corresponding author: Sangeetha S.; *Email:** sangeets2@srmist.edu.in

Received: 24 Jul 2024, Revised and Accepted: 16 Nov 2024

ABSTRACT

Objective: This study aims to develop a new lipid formulation known as Solid Lipid Nanoparticles (SLNs) to increase the oral bioavailability of Nirmatrelvir (NMT) by facilitating intestinal lymphatic transport. Nirmatrelvir is a crucial antiviral agent utilized for the treatment and prophylaxis of Coronavirus disease 2019 (COVID-19).

Methods: Nirmatrelvir loaded solid lipid nanoparticles (NMT-SLNs) were formulated using the microemulsion technique with compritol 888 ATO, and the optimization of lipid and surfactant concentrations, as well as homogenization time, was achieved through the box-behnken design. The resulting NMT-SLNs underwent evaluation for percentage entrapment efficiency, Particle diameter, Zeta potential, Polydispersity index (PDI), and *In vitro* drug release studies.

Results: Optimized formulation (NF8), yielded a particle of 183.26±2.12 nm size with a narrow distribution of 0.071±0.004PDI, negative zeta potential of-24.63±1.92 mV, percent entrapment of 86.94±2.08%, and cumulative drug release of 84.42±3.16% over 24 h. Furthermore, solid-state characterization by PXRD, surface morphology assessment by SEM, and an *in vivo* distribution study employing albino wistar rats were conducted. The findings demonstrated a 10.14-fold increase in relative bioavailability and an 85% enhancement in brain uptake compared to pure NMT solution following oral administration.

Conclusion: This research highlights the potential advantages of solid lipid nanoparticles (SLNs) in enhancing the oral delivery of nirmatrelvir. finally, the study concluded that SLNs serve as a promising vehicle for improving bioavailability and facilitating effective brain delivery.

Keywords: Solid lipid nanoparticles, Anti-viral agent, Paxlovid™, Nirmatrelvir, Compritol 888 ATO, Box-behnken design, Risk assessment analysis

DOI: https://dx.doi.org/10.22159/ijap.2025v17i1.52380 Journal homepage: https://innovareacademics.in/journals/index.php/ijap

INTRODUCTION

Nirmatrelvir, an antiviral drug [1] developed by Pfizer [2], secured its initial emergency use authorization from the USFDA (United States Food and Drug Administration) on December 22, 2021 [3], for the control of COVID-19, the worldwide pandemic spurred through SARS-CoV-2 (Severe Acute Respiratory Syndrome Coronavirus 2) [4]. When utilized in conjunction with Ritonavir under the brand name "Paxlovid™," [5] it serves to address mild to moderate COVID-19 and mitigate the heightened risk of progression to severe COVID-19 [6]. Nirmatrelvir acts as a potential inhibitor of Mpro [7], the primary protease of SARS-CoV-2, essential for viral replication [8, 9]. Notably, while being the first oral antiviral medication for COVID-19, Nirmatrelvir exhibits low oral bioavailability (34%-50% in Rats, 8.5% in Monkeys) [10], undergoing extensive first-pass metabolism by CYP3A in liver microsomes and oxidative metabolism within the GI tract, potentially resulting in therapeutic inadequacy. Consequently, co-administration of a low dose of Ritonavir is recommended to address this challenge [11].

Ritonavir, which is one of the components of Paxlovid™ (a combination of Nirmatrelvir and Ritonavir tablets), inhibits the CYP3A enzyme, slowing down the breakdown of Nirmatrelvir and increasing its half-life to 5-6 h [12, 13]. If Nirmatrelvir is not taken together with Ritonavir, its plasma levels will be too low to have the intended therapeutic effect [11, 14]. However, taking Nirmatrelvir with Ritonavir can lead to significant interactions with other drugs. As a CYP3A inhibitor, Ritonavir can elevate the plasma levels of co-administered drugs that are also metabolized by CYP3A, potentially causing serious and life-threatening reactions [15]. Ritonavir is also known to be associated with liver and kidney toxicity, as well as hypersensitivity reactions [16, 17]. Additionally, Nirmatrelvir plus Ritonavir should not be used in patients taking strong CYP3A enzyme inductors, as this can significantly reduce Nirmatrelvir plasma levels, leading to reduced virologic response and potential drug resistance [18-20]. These findings have led to the development of a new formulation to bypass liver metabolism and improve oral absorption.

An effective approach to address the challenges above involves developing a novel colloidal carrier system capable of accessing systemic circulation via lymphatic transport and bypassing hepatic metabolism [21]. In recent years, Solid Lipid Nanoparticles (SLNs) have garnered significant attention due to their distinct advantages, including small particle size, enhanced drug stability, improved bioavailability, evasion of first-pass metabolism, protection against enzymatic metabolism, the capacity to transport both hydrophilic and lipophilic drugs, and ease of large-scale production [22]. Furthermore, SLNs not only consolidate the benefits of colloidal carrier systems such as Liposomes, Polymeric Nanoparticles (NPs), and Fat Emulsions but also circumvent the limitations associated with these systems [23]. In comparison to polymeric NPs, SLNs demonstrate biodegradability and biocompatibility, provide sustained release arising from drug immobility within solid lipids, and exhibit superior physical and chemical stability over liposomes [24]. Additionally, SLNs advance drug bioavailability through lymphatic uptake, as lipid particulate systems engage with intestinal enterocytes to form chylomicrons that bypass hepatic first-pass metabolism upon secretion into the lymphatic circulation [25].

The primary objectives of the current research endeavor centered on the formulation of Nirmatrelvir loaded Solid Lipid Nanoparticles (NMT-SLNs) through the utilization of microemulsion technique, followed by an optimization process. A Box-Behnken design was adopted to optimize and examine the impact of various formulation and process factors on critical quality measures, notably particle diameter, and efficiency of entrapment (%EE). Diverse characterization studies have been conducted to assess the shape, surface morphology, and drug release kinetics. Moreover, the investigation encompassed the establishment of rat animal models to explore the Pharmacokinetics and Tissue distribution of NMT-SLNs.

MATERIALS AND METHODS

Materials

MSN Laboratories Pvt. Ltd., Hyderabad, India, provided complimentary samples of Nirmatrelvir (NMT) and Compritol 888 ATO. Stearic acid, Glyceryl monostearate, Poloxamer 188, and Poloxamer 407 are bought from Sigma Aldrich, Mumbai, India. Soya lecithin was procured from "Loba Chemie Pvt Ltd.", Mumbai, India. Dialysis membrane (Mol. Wt cut-off 12000-14000dlts) was purchased from "HiMedia Laboratories Pvt. Ltd", Mumbai, India. Syringe filters of nylon (0.45 µm Pore size, 25 mm diameter) were brought from Labsoul, India. Laboratory animals (Albino Wistar rats) were procured from Mahaveera Enterprises, Hyderabad, India. HPL-grade solvents like Water, Acetonitrile, and Methanol were supplied by Merck Ltd., Mumbai, India. Analytical-grade chemicals and solvents were utilized in all other cases.

Methods

Screening of lipid and surfactant phase

The choice of lipid depends on the drug's maximum solubility. A solubility study was conducted by adding precisely weighed 5 mg of NMT to 1 gm of melted lipid, which was heated 10 °C above its melting point with continuous stirring until a clear solution was achieved. Subsequently, incremental amounts of the drug, in 5 mg portions, were added under continuous stirring until failed, despite agitation for a full day, to dissolve in the molten lipid. The assessment of solubility relied on visual observation, with the appearance of a turbid solution indicating the endpoint. The Lipid showing the greatest solubility for the drug is identified as having the maximum drug loading capacity and was thus chosen for further formulation investigation [26].

The surfactant selection process was based on the evaluation of average particle diameter and percent entrapment efficiency (%EE). NMT-SLNs trial batches were prepared using a pre-selected lipid and various surfactant systems. Subsequently, the resulting SLN dispersions underwent analysis to determine particle dimensions and entrapment efficiency (%EE). The criteria used in surfactant selection were the ability to encapsulate the largest amount of the drug and to produce the smallest particle size. The surfactant demonstrating these characteristics was chosen for further formulation development [27].

Drug-excipients compatibility study

Compatibility assessments were conducted using Fourier Transform Infrared Spectroscopy (FTIR) to ascertain if there was any incompatibility between the drug and selected excipients. FTIR spectra of the drug Nirmatrelvir and the physical mixture comprising the drug with selected excipients were recorded after subjecting them to stress conditions of 7 d at 25 °C and 60%±5% RH in the range of 4000-400 cm^{-1}. Subsequently, the resulting spectrum was scrutinized for any noteworthy alterations [28].

Risk assessment analysis

The Ishikawa (Fishbone) diagram, presented in fig. 1, was utilized to conduct a risk assessment aimed at identifying potential causes of product variability during the development of NMT-SLNs. Table 1 provides a comprehensive overview of the risk assessment analysis, encompassing components, including the quality target product profile and critical quality attributes [29].

Table 1: Components of quality target product profile (QTPP) and critical quality attributes (CQA) required for formulation of NMT-SLNs

Quality target product profile (QTPPs)		
QTPPs	**Target**	**Justification**
Drug delivery system	Solid lipid nanoparticles	Improved bioavailability in the oral route, Increased tissue accumulation (Brain-important reservoir site for viruses)
Dosage type	Controlled release	Prolonged therapy with the minimum possible dose
Route of administration	Oral	Improved patient compliance
Drug release	up to 80% in 24 h	Improves intensity of drug action
Critical quality attributes (CQAs)		
CQAs	Target	Justification
Average particle diameter	Less than 200 nm	Offers lymphatic uptake bypass phagocytosis by reticular endothelial system (RES)
Percentage entrapment efficiency	More than 80%	Increased drug loading offers an efficient pharmacological response

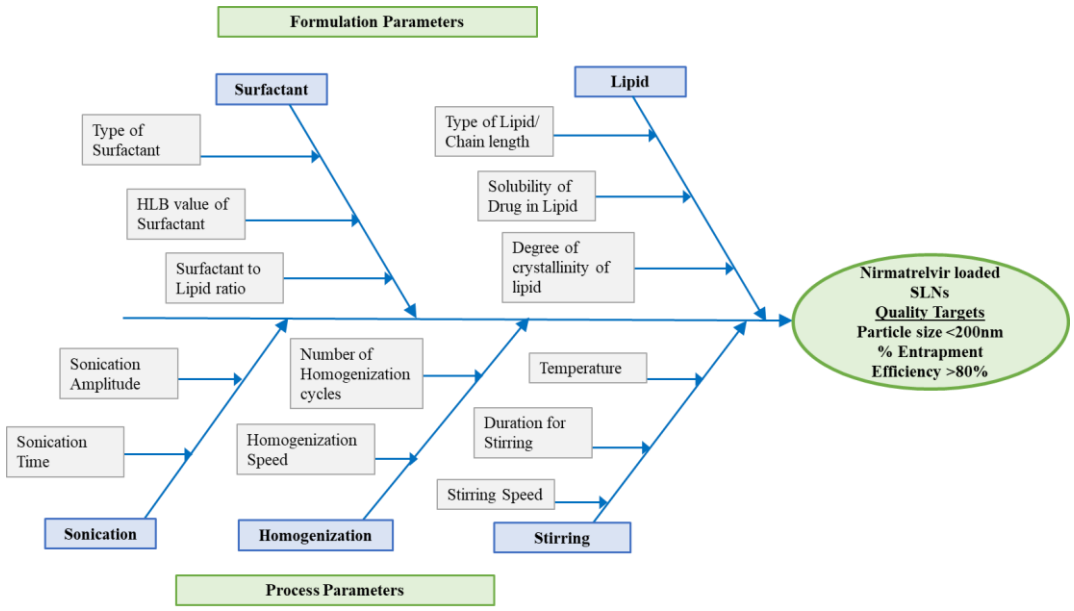

Fig. 1: Ishikawa/Fishbone diagram for risk assessment in the development of NMT loaded SLNs

Experimental design

Box-Behnken Design (BBD) featuring 3-factors and 3-levels, entailing 15 experimental runs, including 3 Center Points, was utilized for the optimization study [30]. The trial version of Design-Expert software (STAT-EASE 360) facilitated this process. Independent variables namely Concentration of Lipid (X1), Concentration of Surfactant (X2), and Homogenization time (X3) were deliberately set at low, medium, and high levels to gauge their impact on two responses: particle size and percent entrapment. The primary goal of optimizing NMT-SLN formulae is to reduce particle size while increasing entrapment efficiency. Furthermore, ANOVA was utilized to statistically validate the polynomial equations specified by Design-Expert Software. Table 2 provides the experimental formulas and their respective codes. The levels for lipid were defined as 5%, 7.5%, and 10%, for surfactant as 1%, 1.5%, and 2%, and for homogenization times as 30, 60, and 90 min.

Table 2: Formulation codes and their compositions for the development of NMT-SLNs using box-behnken design

No of runs	Formulation code	Factor 1 (X_1-Lipid, %w/v)	Factor 2 (X_2-surfactant, %w/v)	Factor 3 (X_3-homogenization time, min)
1	NF1	7.5	1	3
2	NF2	7.5	1.5	2
3	NF3	5	1.5	1
4	NF4	7.5	1	1
5	NF5	10	1	2
6	NF6	5	1.5	3
7	NF7	7.5	1.5	2
8	NF8	5	2	2
9	NF9	10	2	2
10	NF10	5	1	2
11	NF11	10	1.5	1
12	NF12	7.5	2	3
13	NF13	10	1.5	3
14	NF14	7.5	2	1
15	NF15	7.5	1.5	2

Method of preparation

Nirmatrelvir-loaded solid lipid nanoparticles (NMT-SLNs) were developed utilizing the previously reported microemulsion technique [31] employing pre-screened lipid and surfactant systems, namely Compritol and Poloxamer 188. In total, fifteen formulations were prepared based on the BBD with the changes in lipid and surfactant concentrations and the number of homogenization cycles as presented in table 1. First, the lipid phase (Compritol) was melted at 75-80 °C, which is slightly above its melting point of 70 °C and then NMT was added. At the same time, the aqueous phase containing the surfactant (Poloxamer 188) was also heated to the same temperature. The hot aqueous phase was then mixed with the molten lipid phase to obtain the primary emulsion, which was stirred magnetically at 500 rpm for 10-15 min. The resultant hot emulsion was incrementally added into ice-cold water with continuous homogenization at 20,000 rpm for a specified period based on BBD. The resulting NMT-SLNs underwent additional size reduction to the nanoscale through Probe Sonication for 10 min. Subsequently, the prepared NMT-SLN dispersions were stored undisturbed at 4 °C until further analysis.

Characterization of formulated NMT-SLNs

Particle size and polydispersity index (PDI)

The average particle diameter and PDI of NMT-loaded solid lipid nanoparticles (NMT-SLNs) were determined using a Particle Size Analyzer (Nanoparticle Size Analyzer SZ-100Z, Horiba Ltd., Japan). Before measurement, all formulations were diluted to an appropriate concentration using double distilled water. The samples were subsequently analyzed by placing them in disposable cuvettes, and the results for particle size and PDI were recorded in triplicate [32].

Zeta potential

The surface charge of NMT-SLNs was assessed through Zeta potential measurements. The measurements were conducted in triplicate using the same instrument, employing an electric field strength of 23V/cm at a temperature of 25 °C [33].

Entrapment efficiency

The percentage entrapment efficiency of NMT-SLNs was evaluated by the centrifugation method with High-Speed Cooling Centrifuge (Remi Instruments, Ltd., Mumbai, India) to quantify the free drug in an aqueous medium. The encapsulation efficiency of the drug in SLNs was determined as the difference between the total drug used in preparing SLNs and the amount of drug that leached in the supernatant. A certain volume of NMT-SLNs dispersion was taken in a centrifugation tube and centrifuged at 12000 rpm for 20 min at 40 °C. Subsequently, the supernatant was collected and diluted and the concentration of the free drug was then quantified using a UV-Visible spectrophotometer with λ max 262 nm [34]. The entrapment efficiency was then determined using the formula that was provided in the prescription.

$$\text{“\% Entrapment efficiency}= \frac{\text{Total amount of the drug in formulation}-\text{Amount of the drug in supernatant}}{\text{Total drug content}} \times 100\text{”}$$

Optimization of variables

For all formulations prepared using the box-behnken design, an optimization process was employed to determine the optimal levels of lipid, surfactant, and homogenization time. This optimization was based on two critical quality attributes: particle size and Entrapment Efficiency. Statistical analysis of data including ANOVA, model equation generation, and contour plot construction for each response, was conducted using the STAT-EASE 360 trial version. Furthermore, to determine the relation between the independent and dependent variables, three-dimensional (3D) surface plots were adopted. To optimize NMT-SLN formulations, the desirability function was set to minimize particle size while maximizing entrapment efficiency.

***In vitro* drug release studies**

Drug release studies for NMT-SLNs were carried out using the dialysis membrane diffusion method. A dialysis membrane with a molecular weight cut-off of 12,000-14,000 Da was placed in the release medium for 16 h, and then placed over a diffusion glass vial and clamped at both ends. A specific volume of the NMT-SLNs dispersion containing an equivalent of 10 mg of the drug was transferred to a dialysis tube and immersed in 100 ml of the diffusion medium in a beaker. The medium was maintained at 37±0.5 °C using a magnetic stirrer (REMI 2MLH) with stirring at 100 rpm and continuous stirring. The dissolution was performed in simulated gastric fluid (pH 1.2) for the first 2hours and then, in simulated intestinal fluid (pH 6.8) for a further 22 h. After the specified time, 2 ml of the samples were collected and replaced with the buffer to maintain sink conditions. All the samples were

measured using a UV-visible spectrophotometer at 262 nm, and the percent drug release was determined using the formula.

$$\% \text{ Drug release} = \frac{\text{Concentration} \times \text{Dilution Factor} \times \text{Vol. of Dissolution medium}}{1000} \times 100$$

Solid-state characterization by XRD

X-ray diffraction (XRD) analysis was conducted to determine the crystalline nature of Nirmatrelvir (NMT) in the formulated SLNs. The XRD patterns of Nirmatrelvir, the physical mixture, and the optimized SLN formulation were recorded using an X-ray diffractometer (Rigaku Mini Flex 600, Rigaku Corporation, Japan). The analysis employed a generator with a Cu anode at 40kV voltage and 15mA current. All the samples were subjected to Cu-K alpha radiation at the 2θ angle of 30 to 90 with an increment rate. It is recommended to take 0.0200 degrees per step [36]. After that, the obtained PXRD patterns were compared with the characteristic peak intensity related to Nirmatrelvir.

Surface morphology by scanning electron microscopy

The optimized dispersion of NMT-SLNs (NF8) was further examined for its shape and surface morphology using scanning electron microscopy (SEM) with the help of VEGA 3, SBH, TESCAN Brno S. R. O, Czech Republic. In summary, the sample was gold coated and the SEM analysis was carried out at an accelerating voltage of 15 kV with different magnifications [37].

***In vivo* characterization**

Study protocol and experimental procedure

Albino Wistar rats chosen for the study were procured from Mahaveera Enterprises, Hyderabad, India, and the method that was proposed for this study was approved by the Hindu College of Pharmacy Institutional Animal Ethics Committee (IAEC) in Andhra Pradesh, India with the reference number IAEC-HCOP/2022/07. All the rats were acclimatized in the animal house for 7 d and maintained on 12 h light/dark cycle at a controlled temperature of 24±2 °C/60±5%RH with access to food and water ad libitum. Eighteen rats of 200-250 gs body weight were selected and were starved overnight before the experiment. Rats were randomly divided into three groups with each group comprising six animals (6). Group I was administered with a pure Nirmatrelvir solution at a dose of 10 mg/kg body weight, Group II was administered with the optimized NMT-SLNs formulation NF8 at the same dose of 10 mg/kg body weight and Group III was given solvent control in the form of sterile buffer of pH 7.4. Blood samples (0. 5 ml) were withdrawn from the retro-orbital plexus through glass capillaries at time intervals of 0, 0. 5, 1, 2, 3, 6, 12, 18, and 24 h. The collected samples were then placed in heparinized microtubes and centrifuged at 5000 rpm for 10 min at 40 °C. Following centrifugation, 100µl of supernatant plasma was separated and subjected to analysis using a standardized HPLC method [38, 39].

Pharmacokinetic studies

Pharmacokinetics of Nirmatrelvir were assessed by the determination of Cmax, Tmax, AUC, K, t1/2, and MRT by non-compartmental analysis [38]. To assess the statistical significance of the results, a student's t-test was used with a significance level of less than 0.05 ($p<0.05$) was considered significant. Cmax and Tmax were read directly from the Cp versus T graph. The Area Under the Curve (AUC) was performed with the help of the trapezoidal rule of the linear logarithmic type. The K_E and $t_{1/2}$ were determined from the elimination phase of the Plasma Concentration vs Time graph. Relative bioavailability was assessed by comparing the $AUC_{0-\infty}$ of NMT-SLNs with that of $AUC_{0-\infty}$ of NMT pure solution, utilizing a defined formula.

$$\text{Relative Bioavailability} = \frac{[\text{AUC}] \text{ of test} \times \text{Dose of Control}}{[\text{AUC}] \text{ of control} \times \text{Dose of Test}} \times 100$$

Tissue distribution

Studies at 24 h post-treatment, the rats were sacrificed by cervical dislocation, and their liver, spleen, lungs, kidneys, heart, and brain organs were harvested, washed with saline solution and immediately stored at-20 °C until analysis. Each organ was homogenized separately with the help of a tissue homogenizer (Remi Motors Ltd., Mumbai, India), and the homogenate was then centrifuged at 15000 rpm for 30 min [39]. The supernatant was then collected and filtered through 0.45 µm nylon filters and analyzed after appropriate dilution with phosphate buffer solution, according to the described HPLC method.

Statistical analysis

The pharmacokinetic study's findings were presented as mean+/- standard deviation (SD). The significance of the difference between the formulations was evaluated at a level of $P<0.05$ using the student t-test.

Stability studies

An NMT-SLNs (NF8) formulation's stability was tested by measuring fluctuations in the size of particles, zeta potential, as well as percent entrapment. This testing was carried out using a stability chamber manufactured by Inlab Equipment, India. The NMT-SLNs (NF8) suspension was packaged in screw-capped amber glass bottles and subsequently stored under three distinct conditions: "5±3 °C, 25±2 °C/65±5%RH, and 40±2 °C/75±5%RH" for 90 d. Samples were retrieved at intervals of 1, 30, 60, and 90 d during the storage period and subjected to evaluation for average particle diameter, PDI, ZP, and %EE. The ensuing results were subsequently scrutinized to discern any noteworthy alterations [40].

RESULTS AND DISCUSSION

Screening of lipid and surfactant phase

Solubility of the drug within the lipid matrix played a crucial role as it directly impacted the drug loading capacity. An assessment of Nirmatrelvir's solubility in four distinct lipids-Tripalmitin, Glyceryl monostearate (GMS), Stearic acid (SA), and Compritol-was conducted, with the results depicted in fig. 2. The solubility trend of Nirmatrelvir in these lipids was as follows: Compritol>GMS>SA>Tripalmitin. Among the lipids examined, Compritol demonstrated the highest solubility for Nirmatrelvir (235 mg/1g of lipid), followed by Glyceryl monostearate (170 mg/1g of lipid). The results are similar to the findings of Priyanka *et al.*, who reported Compritol showed entrapment for montelukast SLNs compared to GMS and stearic acid [33]. Compritol, classified as an acyl glyceride and comprising mono-, di-, and triglycerides of Behenic acid [41, 42], yields less ordered crystals, allowing for increased accommodation of the drug. This notably high solubility makes Compritol the preferred lipid phase.

Inclusion of a surfactant is pivotal in achieving a stable formulation, as solid lipid nanoparticles constitute colloidal systems comprising solid lipids dispersed in an aqueous medium in conjunction with a surfactant. A selection process was undertaken involving four distinct surfactants, namely Span 60, Tween 80, Poloxamer 407, and Poloxamer 188, based on criteria that would yield the smallest particle size and the highest entrapment efficiency. The outcomes, illustrated in fig. 2, indicated Poloxamer 188 to be the most effective in achieving reduced particle size and increased entrapment efficiency, followed by Tween 80, Poloxamer 407, and Span 60, in respective order. These results were in good agreement with those obtained by Ekambaram *et al.*, who found the highest entrapment efficiency of Ramipril SLNs in case of Poloxamer-188 than tween 80 and span 60 [43]. Effective attributes of Poloxamer 188, such as its relatively lower molecular weight and higher HLB (Hydrophilic Lipophilic Balance) value compared to other surfactants, likely contributed to the resulting minimum particle size and maximum entrapment efficiency. Additionally, considering its Generally Recognized as Safe (GRAS) status [44], Poloxamer 188 was deemed the optimal surfactant for formulating NMT-SLNs.

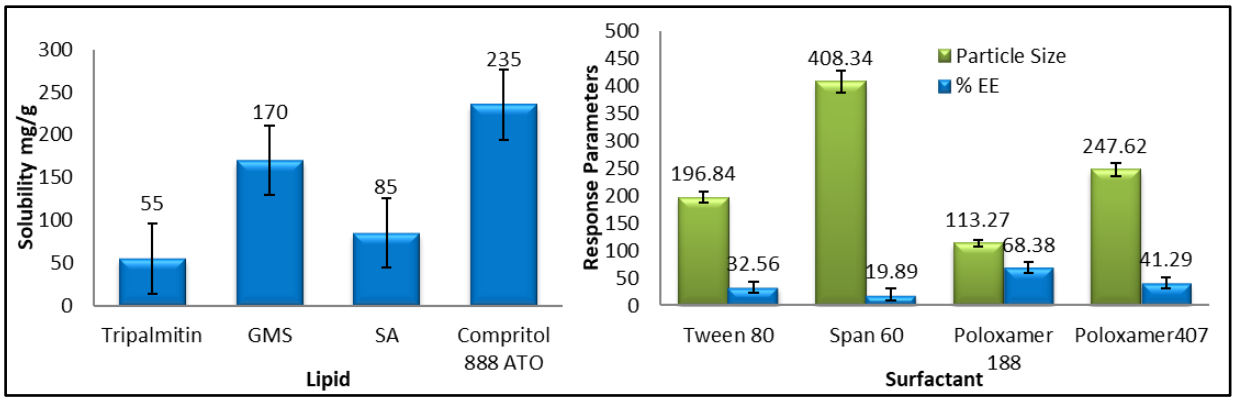

Fig. 2: Screening of lipid and surfactant to formulate NMT-SLNs (GMS-glyceryl monostearate, SA-Stearic acid, %EE-percentage entrapment efficiency)

Drug-excipients compatibility study

The FTIR spectra of pure Nirmatrelvir and Physical mixture (NMT+Compritol+Poloxamer-188) are depicted in fig. 3. The IR spectrum of Nirmatrelvir reveals characteristic peaks at the following wave numbers: The functional groups identified in the spectrum include; O-H stretching at 3317 cm^{-1}, C-H stretching at 2918 cm^{-1}, C=N stretching at 1647 cm^{-1}, N-H bending at 1517 cm^{-1}, C=C stretching at 1426 cm^{-1}, C=S stretching at 1153 cm^{-1} and C-H bending at 709 cm^{-1}. When comparing these spectra, it can be seen that there is no shift or any missing functional peaks in the spectrum of the physical mixture. This proves that there are no chemical incompatibilities between the Nirmatrelvir and the selected excipients.

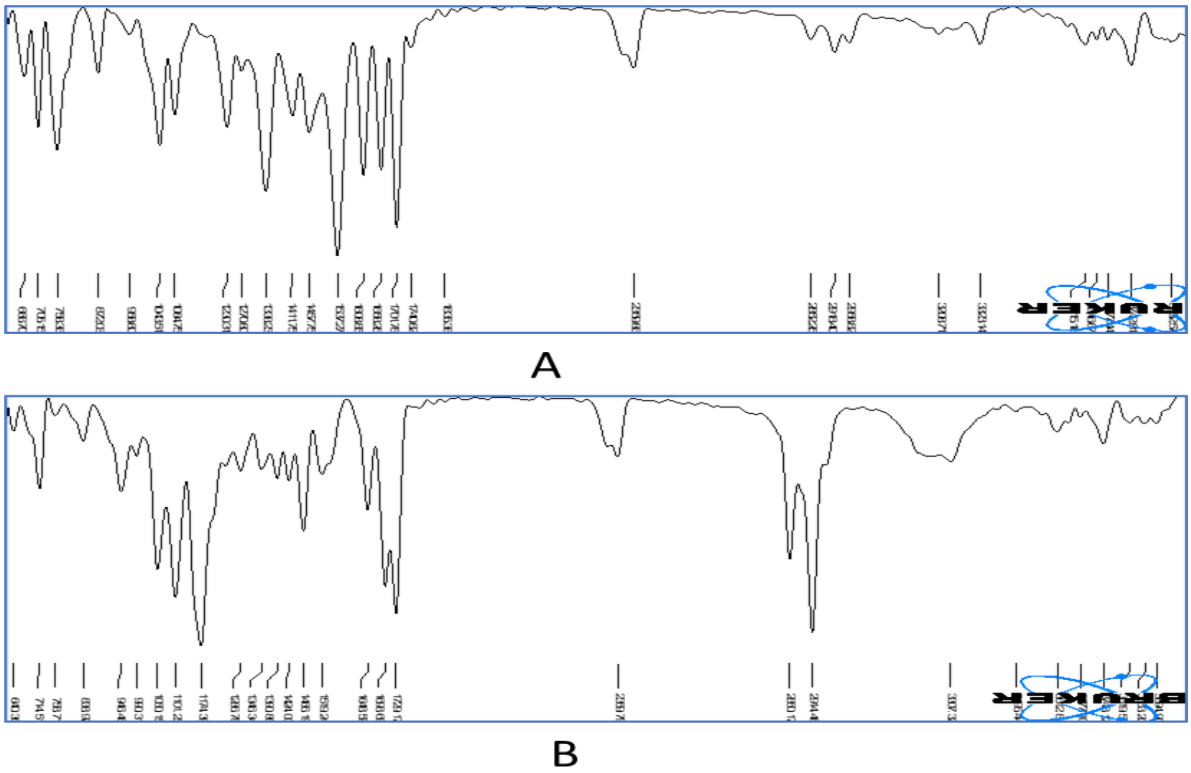

Fig. 3: FTIR spectra of A) Nirmatrelvir and B) Physical mixture (Nirmatrelvir+Compritol 888 ATO+poloxamer 188)

Characterization of formulated NMT-SLNs

By the box-behnken design, a total of 15 formulations of NMT-SLNs were developed and evaluated as specified in the methodology

Particle size (PS) and polydispersity index (PDI)

The findings of the particle size and size distribution analysis are outlined in table 3. The average particle diameter and distribution index of NMT-SLNs ranged from 183.26±12.58 to 913.56±37.18 nm and 0.071±0.012 to 0.352±0.16, respectively.

All dispersions of NMT-SLNs demonstrated an average particle size below 1000 nm, with the attainable size being notably influenced by formulation variables, specifically the concentration of lipid and emulsifier. Literature highlights the preferential transport of SLNs via the lymphatic system and emphasizes the importance of maintaining a size below 200 nm to evade uptake by the Reticular Endothelial System (RES) [45]. This parameter warrants consideration during the optimization of formulations. The Polydispersity Index (PDI) serves as a metric for evaluating particle size distribution, with a maximum PDI of 0.5 deemed optimal for nanoparticles. Generally, a lower PDI

reflects a narrower particle size distribution. Notably, all NMT-SLN formulations exhibited PDI values below 0.5, indicating a narrow particle size distribution. This was similar to the study reports of Qushawy *et al.*, where the prepared Carbamazepine SLNs had a narrow size distribution with PDI ranging from 0196±0.05 to 0.419±0.02, which is less than 0.5 [46].

Zeta potential

The results of the Zeta potential analysis are presented in table 3, which shows the values ranging between-18. 6±5.4 to-36.7±8. 1 mV. Zeta potential represents a critical physicochemical parameter impacting the stability of formulations. A minimum ZP of ±20 mV is deemed favorable for ensuring the optimal stability of nanoparticles [47]. All NMT-SLN formulations were meticulously engineered to exhibit a negative zeta potential surpassing 20 mV, attributable to the intrinsic chemical composition of the lipid and surfactant utilized, thereby signifying resilience against particle aggregation.

Percentage entrapment efficiency

The findings of the Entrapment Efficiency analysis are delineated in table 3. The Entrapment Efficiency (%EE) of NMT-SLNs ranged from 84.63% to 98.62%. It is noteworthy that the lipophilic properties of Nirmatrelvir [48] significantly contributed to the entrapment, accounting for more than 80% of the reported efficiency.

Table 3: Batch-to-batch evaluation data for average particle size, PDI, zeta potential, and % entrapment efficiency of NMT-loaded SLNs

Formulation code	Particle size (Response 1-Y_1) (nm)	PDI	Zeta potential (mV)	Entrapment efficiency (Response 2-Y_2) (%)
NF1	589.75±11.02	0.306±0.035	-26.94±5.38	80.12±4.16
NF2	419.82±4.17	0.192±0.009	-28.18±2.04	90.63±2.08
NF3	249.26±8.29	0.126±0.015	-22.62±1.12	81.89±2.37
NF4	471.52±7.34	0.261±0.023	-27.52±1.28	87.61±1.98
NF5	854.23±5.21	0.279±0.004	-34.29±2.42	96.24±1.34
NF6	298.15±12.56	0.238±0.024	-22.81±4.16	79.36±3.74
NF7	423.86±3.64	0.181±0.018	-28.96±2.13	94.31±1.94
NF8	183.26±2.12	0.071±0.004	-24.63±1.92	86.94±2.08
NF9	806.45±4.76	0.202±0.012	-36.74±2.05	98.48±1.83
NF10	254.31±5.16	0.197±0.070	-18.67±1.96	80.19±2.27
NF11	807.14±5.45	0.314±0.037	-35.15±2.36	92.85±1.88
NF12	540.13±3.97	0.324±0.027	-30.64±4.89	88.71±3.97
NF13	913.56±2.65	0.352±0.112	-34.91±4.14	86.92±3.93
NF14	556.21±5.27	0.296±0.045	-31.28±1.14	90.42±2.18
NF15	421.42±3.17	0.189±0.006	-28.74±2.56	91.35±1.14

Note: PDI-Polydispersity index, mean±SD (n=3)

Optimization data analysis and experimental validation

The experimental results were analyzed by fitting all fifteen formulations' responses to various models using the trial version of Design Expert Software (STAT-EASE 360). Among these, quadratic models were determined to be the most suitable for the tested parameters, specifically the mean size of particle and % efficiency of entrapment. Below are the equations for quadratics computed for the selected response.

Particle Size (Y_1) =+180.54429+126.66698 X_1-291.40972 X_2-0.202037 X_3-11.67778 X_1X_2-0.001296 X_1X_3+0.075833 X_2X_3-2.09877 X_1^2+85.35000 X_2^2+0.002639 X_3^2

Entrapment Efficiency (Y_2) =-45.30478+18.60262 X_1+40.23500X_2+0.769542X_3-1.49000X_1X_2-0.009167X_1X_3-0.045833X_2X_3-0.927840X_1^2-6.37125X_2^2-0.006565X_3^2

In the specified context, the codes "X1, X2, and X3" are assigned to independent variables, namely Lipid, Surfactant concentration, and Homogenization time, in respective order.

The ANOVA results for the quadratic model relating to particle size (response I) and Entrapment Efficiency (response II) are presented in table 4. The ANOVA for Particle Size yielded an F-value of 14.48, indicating the model's overall significance. Furthermore, the significance of the model's individual term is supported by a P-value of less than 0.05. Similarly, the ANOVA for Entrapment Efficiency demonstrated a model F-value of 86.11, affirming the model's overall significance, with individual terms also exhibiting significance ($P<0.05$). The high R^2values of 0.9776 and 0.9962 for particle size and entrapment efficiency, respectively, signify a strong correspondence between the formulation variables and response parameters.

Table 4: Summary of regression analysis and analysis of variance for response I (Particle size) and response II (% Entrapment efficiency)

Parameters	DF	SS	MS	F	P-value	R^2	SD	CV	Outcome
Particle size									
Model	9	1.031E+06	2.062E+05	14.48	0.0014	0.9776	91.04	19.06	Significant
Residual	3	99716.77	4245.25	-	-	-	-	-	
Total	12	1.131E+06	12.21	-	-	-	-	-	
% Entrapment efficiency									
Model	9	2493.78	498.76	86.11	0.0017	0.9962	2.57	4.11	Significant
Residual	3	29.44	6.59	-	-	-	-	-	
Total	12	2523.22	-	-	-	-	-	-	

Further, the association between independent and dependent variables was examined through the construction of 3D-response surface plots. Design-Expert software generated three-dimensional (3D) response surface graphs representing the analyzed responses, namely particle size and entrapment efficiency, are depicted in fig. 4. From the graphs A and D, it is evident that there is a direct relationship between lipid concentration and particle size and % entrapment meaning that when the lipid concentration increases the particle size increases and the entrapment efficiency also increases. Similar results were also observed by Remya *et al.*, where they reported that particle size and entrapment efficiency increase linearly with the increase in lipid load. Increased particles size and increased viscosity of the dispersion lead to an increased rate of particle agglomeration. Hence, the lipid content of SLNs dispersion

should not exceed 5% [49] On the other hand, plots B and E present the trends where surfactant concentration is inversely proportional to the particle size and directly proportional to the % entrapment, which implies that increased concentration of surfactant decreases the particle size and increases the entrapment efficiency. The observation was in accordance with results reported by Abdelbary *et al.*, who found that the entrapment efficiency of diazepam in prepared SLNs increased by increasing surfactant concentration [50]. The impact of homogenization time on both parameters varied, precluding a generalized conclusion. Insights derived from 3D surface plots C and F indicate that Particle Size decreases and % Entrapment Efficiency increases up to 60 min for homogenization. After this duration, a further increase in homogenization time to 90 min produces an inverse effect. Similar observations were made by another research group, which found reduced entrapment at higher homogenization cycles for the prepared mometasone furoate SLNs [51].

The solution recommended by the Design-Experiment Software, comprising a lipid concentration of 5%, a surfactant concentration of 2%, and a homogenization time of 60 min, was determined based on the criteria of maximum desirability, which emphasizes the highest entrapping efficiency and the smallest particle size. Subsequently, a verification run was conducted to validate the statistical reliability.

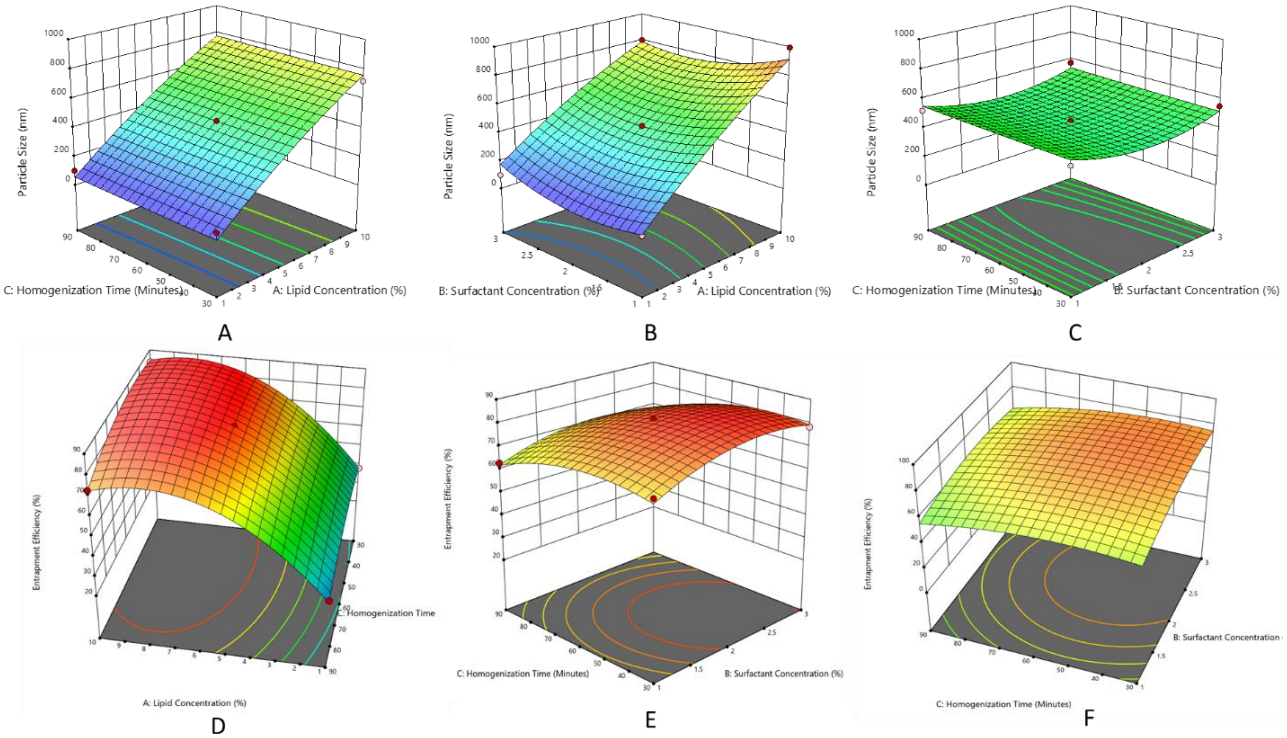

Fig. 4: 3D Surface graphs; A, B and C-depicting the effect of independent variables on response I (Particle Size); D, E and F-depicting the effect of independent variables on response II

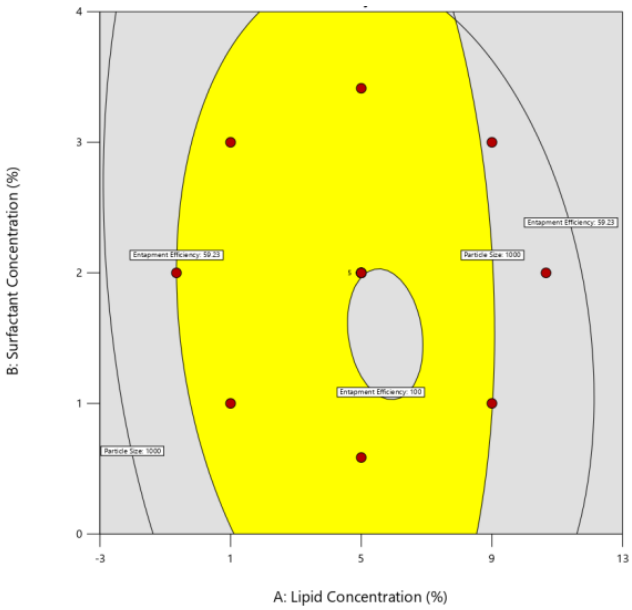

Fig. 5: Overlay plot for optimization of NMT loaded SLNs

The overlay plots depicted in fig. 5 delineate the design space for optimizing NMT-SLNs and proffer recommendations for achieving the desired responses. Subsequently, two verification batches were meticulously prepared and assessed. Table 5 illustrates that the observed values of the checkpoint batches closely aligned with the predicted values, displaying a negligible percentage of bias, thereby affirming the reliability of the optimization procedure.

Table 5: Comparison of observed and predicted values of checkpoint batches for optimization of NMT loaded SLNs

Formulation code	Composition of checkpoint batches			Dependent variables	Observed values	Predicted values	% Bias
	X_1	X_2	X_3				
Batch I	5.6	2.1	64	Particle size (Y_1)	220.43±9.56 nm	218.82 nm	-0.730
				%EE (Y_2)	86.42±4.38%	86.65%	-0.266
Batch II	5.5	2.0	60	Particle size (Y_1)	185.54±7.89 nm	183.96 nm	-0.851
				%EE (Y_2)	85.12±3.72%	84.49%	-0.740

Note: X_1-Lipid, %w/v; X_2-Surfactant, %w/v; X_3-Homogenization Time, min

Drug release studies

In vitro release profiles of NMT solution and NMT-SLN formulations are shown in fig. 6. The release profile of the NMT solution is almost 100% within 5 h and the release of SLNs is spread throughout 24 h. All the formulations of NMT-SLN show a biphasic release profile where the first phase release is about 35-40% in the first 4 h and the second phase release is about 80% in the next 24 h. Similar investigations like biphasic drug release patterns were found and reported for other drugs [33, 47]. The release data were fitted into various kinetic models to establish the mechanism of release. The correlation coefficient of all the NMT-SLN formulations with both the models was high and in the order of First-order model>Higuchi model, thus justifying that the release of the drug is mainly due to diffusion from the lipid matrix. Furthermore, the value of the release exponent of the Korsmeyer-Peppas model was determined to be 0. 89 (n>0. 5), which indicates that non-Fickian diffusion of the drug from NMT-SLNs dispersion [52].

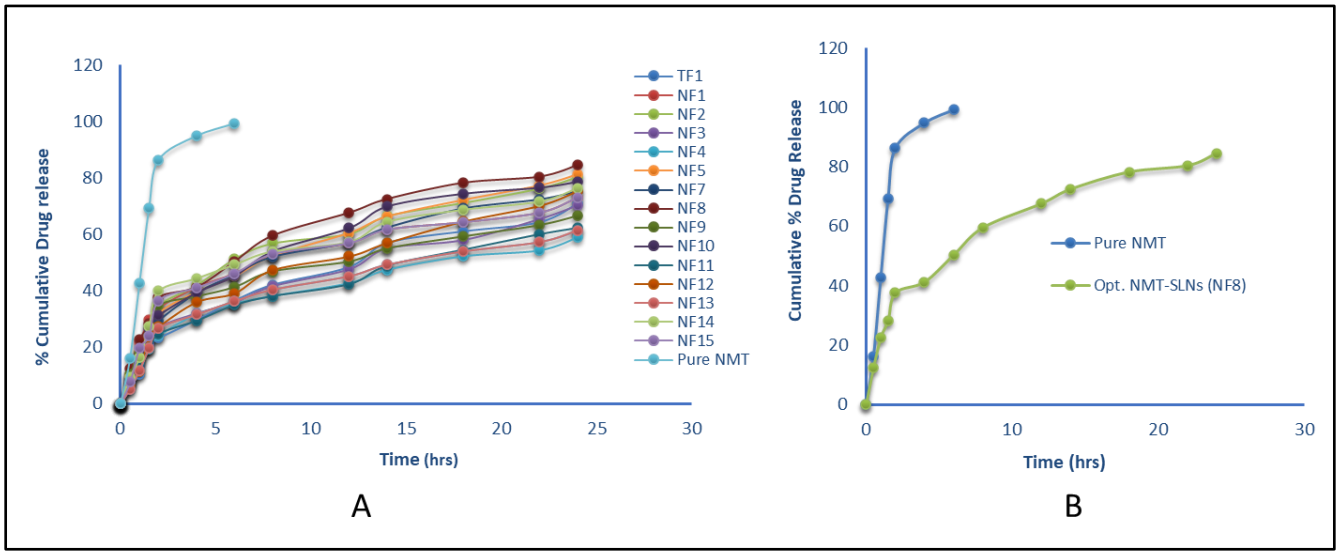

Fig. 6: A-cumulative % drug release VS time plots for NMT-SLNs formulations (NF1-NF15); B-Comparison between *in vitro* release profile of optimized NMT-SLNs (NF8), and NMT solution

Solid state characterization

Powder XRD spectra were utilized and compared. In fig. 7, the X-ray diffractogram of Nirmatrelvir exhibited a series of characteristic sharp peaks at 2 theta scattered angles, confirming the crystalline nature of the drug. These peaks were also present in the physical mixture XRD spectra, signifying compatibility between the drug and excipients. The diffractogram of the optimized NMT-SLNs (NF8) revealed the absence of the majority of peaks and decreased intensity of existing peaks, suggesting a molecular-level dispersion of the drug in the lipid matrix as it transitioned into an amorphous form.

Surface morphology study

The optimized NMT-SLNs formulation (NF8) was analyzed for surface morphology using Scanning Electron Microscopy (SEM). The micrograph in fig. 8 depicts uniformly distributed spherical particles at the nanoscale. The surface exhibits a smooth texture, and there are no signs of particle aggregation.

***In vivo* pharmacokinetic studies**

Table 6 summarizes the kinetic parameters derived using non-compartmental analysis. The data show that Tmax, Cmax, AUC, and MRT values are higher for TNF-loaded SLNs compared to pure Nirmatrelvir, indicating increased bioavailability for compounded NMT-SLNs. The AUC for the Nirmatrelvir solution was 504.16±15.29ng/h/ml, while for "NMT-SLNs" it was 5112.26± 13.42ng/hr/ml. The results revealed that NMT-SLNs had a 10.14-fold improvement in oral bioavailability compared to the Nirmatrelvir solution. The increased bioavailability of SLNs may result from m-cells in the intestinal Peyer's patch absorbing nanoparticles via lymphatic transport, subsequent permeability of nanoparticles across the GI membrane via encapsulation into chylomicrons, and improved paracellular transport due to lipid matrix [53]. All these findings clarified that the pharmacokinetic profile of NMT was significantly ($P<0.05$) improved when formulated into Solid Lipid Nanoparticles (SLNs). Similar findings were reported by another research group Muhammad *et al.*, who found a 5.25-folds increase in Famotidine oral bioavailability when dispersed in SLNs [36].

Table 7 summarizes the concentration of NMT in different organs after oral NMT solution administration and optimized NMT-SLNs dispersion at a single dose comparable to 10 mg/kg body weight. The targeting efficiency of NMT from SLN dispersion was in the following order: Brain, Heart, Lungs, Kidney, Liver, and Spleen, as fig. 9 illustrates. The data showed that NMT-SLNs considerably (>0.5) reduced the absorption of the Reticular Endothelial System (RES), particularly in the Liver and Spleen. This finding may account for part of the NMT-SLNs' increased oral bioavailability. The literature also reports that RES can evade phagocytosis of nanoparticles smaller than 200 nm [54]. Subsequent investigations into tissue distribution also revealed that brain endothelial cells absorbed NMT-SLNs at a greater rate than NMT pure solution. This may be explained by the ease with which nanoparticles can evade membrane-bound P-gp efflux transport and breach the blood-brain barrier. These results are in good agreement with those obtained by Chattopadhyay *et al.*, who observed increased cellular accumulation of Atazanavir when delivered by SLNs [55].

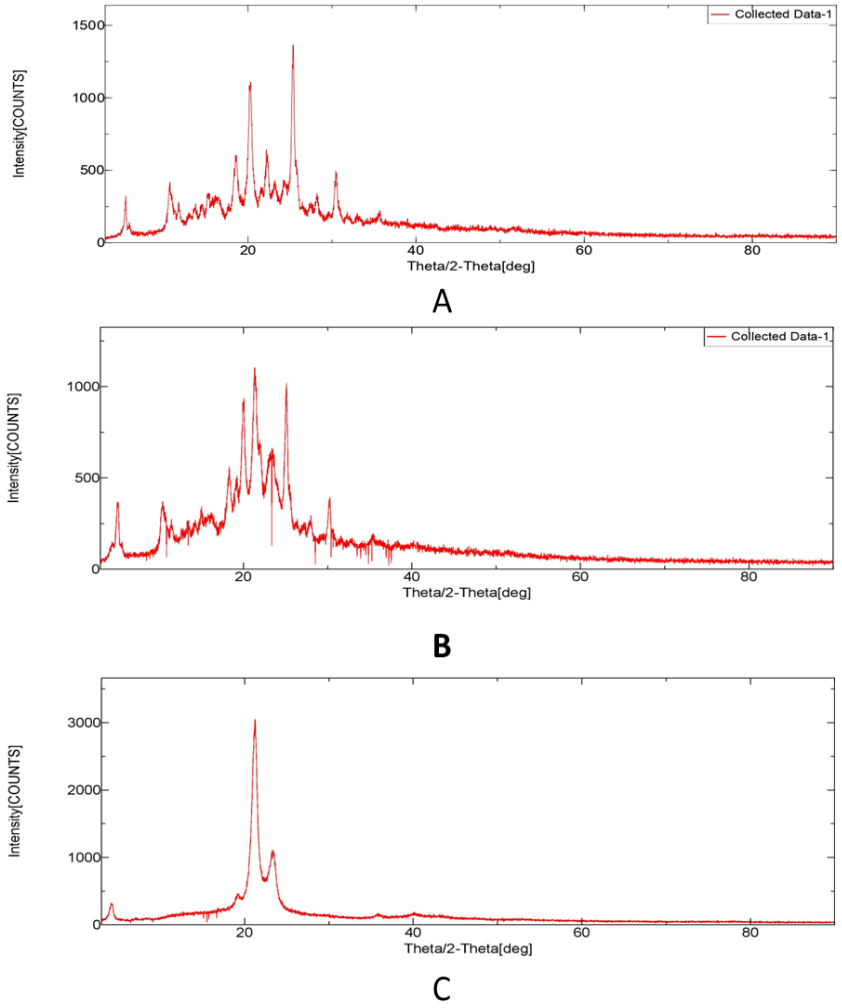

Fig. 7: X-ray diffractograms A) Pure nirmatrelvir, B) Physical mixture and C) Optimized NMT-SLNs formulation (NF8)

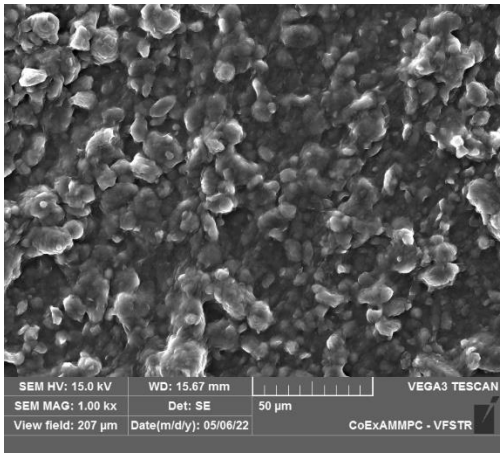

Fig. 8: Scanning electron micrograph of optimized NMT-SLNs formulation (NF8)

Table 6: Pharmacokinetic parameters of pure NMT solution and optimized NMT-SLNs (NF8)

Parameter	Pure NMT solution	Optimized NMT-SLNs (NF8)
Cmax	44.37±3.34ng/ml	223.16± 1.45ng/ml
Tmax	3.0±0.0 h	4.5± 0.5 h
K_a	0.26± 0.21 h^{-1}	1.89±0.026 h^{-1}
K_E	2.37± 0.65 h^{-1}	0.12±0.002 h^{-1}
$t_{1/2}$	6.1± 0.42 h	28. 41±2.35
$[AUC]_{0-\infty}$	504.16±15.29ng/h/ml	5112.26±13.42ng/h/ml
MRT (h)	10.48±1.05 h	36.20± 1.14 h

Note: mean± SD, n=6

Table 7: The findings of the *in vivo* tissue distribution studies of pure NMT solution and optimized NMT-SLNs (NF8)

Organ	Pure TNF solution	Optimized NMT-SLNs (NF8)
Liver	76.42±3.54ng/g	14.02±0.78ng/g
Spleen	112.34±3.22ng/g	12.36±2.03ng/g
Lungs	54.93±5.17ng/g	78.83±2.55ng/g
Kidney	53.74± 5.27ng/g	73.94±0.31ng/g
Heart	22.31±0.24ng/g	84.06± 1.52ng/g
Brain	2.6±0.033ng/g	220.58±1.67ng/g

Note: mean± SD, n=6

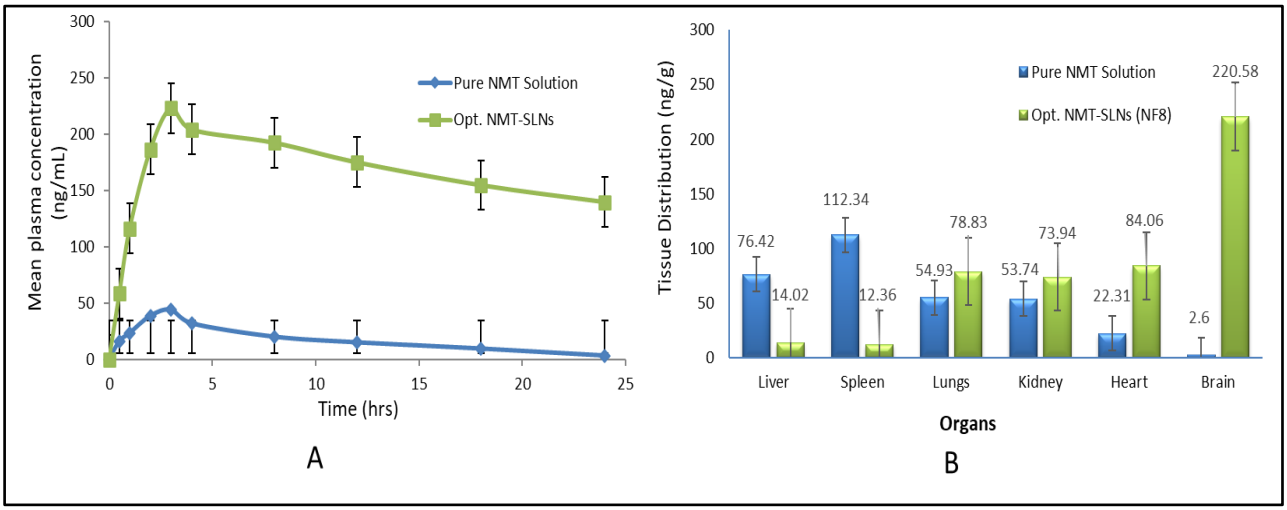

Fig. 9: Pharmacokinetic profile and tissue distribution of NMT on a single oral dose of optimized NMT-SLNs and pure NMT solution (Note: mean±SD, n=6)

Stability studies

The stability of the optimized NMT-SLNs formulation (NF8) was determined under different storage conditions as depicted in table 8 below. During the 6-month stability period at 5±3 °C and 25±2 °C/65±5% RH, no alteration was observed in physical appearance, particle size, PDI, and % entrapment efficiency. However, it was observed that a slight increase in particle size, PDI, and entrapment efficiency was observed at 40±2 °C/75±5% RH, which was considered insignificant. The results suggest that the NMT-SLNs are stable and possess a shelf-life that is quite suitable.

Table 8: Stability studies data for optimized NMT-SLNs formulation (NF8)

Studies data	Parameters	Sampling intervals		
		1 mo	3 mo	6 mo
5±3 °C	Particle size (nm)	183.26±2.12	183.26±2.12	183.26±2.12
	PDI	0.071±0.004	0.071±0.004	0.071±0.004
	%Entrapment efficiency	86.94±2.08	86.94±2.08	86.94±2.08
25±2 °C/65±5%RH	Particle size	183.26±2.12	183.26±2.12	183.26±2.12
	PDI	0.071±0.004	0.071±0.004	0.071±0.004
	%Entrapment efficiency	86.94±2.08	86.94±2.08	86.94±2.08
40±2 °C/75±5%RH	Particle size	183.26±2.12	185.06±2.32	192±2.54
	PDI	0.071±0.004	0.091±0.012	0.093±0.014
	%Entrapment efficiency	86.94±2.08	84.12±1.25	83.92±1.18

Note: mean±SD, n=3

CONCLUSION

Present research has conclusively demonstrated the particular benefit of screening Lipid and Surfactant phases, with all formulations displaying a drug loading exceeding 80%. In this study, solid lipid nanoparticles loaded with nirmatrelvir (MNT-SLNs), an antiviral medication for COVID-19 treatment, were effectively prepared using the microemulsion technique with compritol 888 ATO and optimized by box-Behnken design. The optimized NMT-SLNs formulation (NF8) exhibited a relatively diminutive particle size of 183.26±2.12 nm and a remarkably high entrapment efficiency of 86.94±2.08%. The primary finding to emerge from this research was a 10.14-fold increase in oral bioavailability, alongside a reported 220.58±1.67 ng/g uptake by brain endothelial cells for NMT-SLNs. These outcomes unequivocally underscore the substantial enhancement in the Pharmacokinetic and Bio-distribution characteristics of nirmatrelvir in the Solid Lipid Nanoparticles formulation. Therefore, this study concludes that Solid Lipid Nanoparticles have the potential to serve as bioavailability-enhancing vehicles and effective carriers for brain targeting.

ACKNOWLEDGEMENT

The authors express sincere gratitude to SRM University, Chennai, and "Hindu College of Pharmacy", Guntur for giving essential facilities and technical assistance.

FUNDING

This research did not receive any funding from any public, commercial, or non-profit funding organizations.

AUTHORS CONTRIBUTIONS

Conceptualization and Supervision were conducted by S. Sangeetha, while Methodology and Original draft preparation were handled by M. Sri Rekha. All authors have thoroughly reviewed and endorsed the manuscript.

CONFLICT OF INTERESTS

The authors also report no conflict of interest to the study.

REFERENCES

1. Owen DR, Allerton CM, Anderson AS, Aschenbrenner L, Avery M, Berritt S. An oral SARS-CoV-2 Mpro inhibitor clinical candidate for the treatment of COVID-19. Science. 2021;374(6575):1586-93. doi: 10.1126/science.abl4784, PMID 34726479.
2. Cascella M, Rajnik M, Aleem A. Features evaluation and treatment of coronavirus (COVID-19). In: Treasure Island (FL); 2024. Available from: https://www.ncbi.nlm.nih.gov/books/NBK554776/. [Last accessed on 22 Nov 2024].
3. Simsek Yavuz S, Komsuoglu Celikyurt FI. An update of anti-viral treatment of COVID-19. Turk J Med Sci. 2021;51(SI-1):3372-90. doi: 10.3906/sag-2106-250, PMID 34391321.
4. Pillaiyar T, Manickam M, Namasivayam V, Hayashi Y, Jung SH. An overview of severe acute respiratory syndrome coronavirus (SARS-CoV) 3CL protease inhibitors: peptidomimetics and small molecule chemotherapy. J Med Chem. 2016;59(14):6595-628. doi: 10.1021/acs.jmedchem.5b01461, PMID 26878082.
5. Ledford H. Long COVID treatments: why the world is still waiting. Nature. 2022;608(7922):258-60. doi: 10.1038/d41586-022-02140-w, PMID 35945375.
6. Lamb YN. Correction to: nirmatrelvir plus ritonavir: first approval. Drugs. 2022;82(9):1025. doi: 10.1007/s40265-022-01737-9, PMID 35689762.
7. Rut W, Groborz K, Zhang L, Sun X, Zmudzinski M, Pawlik B. SARS-CoV-2 Mpro inhibitors and activity-based probes for patient sample imaging. Nat Chem Biol. 2021 Feb;17(2):222-8. doi: 10.1038/s41589-020-00689-z, PMID 33093684.
8. Ahmad B, Batool M, Ain QU, Kim MS, Choi S. Exploring the binding mechanism of PF-07321332 SARS-CoV-2 protease inhibitor through molecular dynamics and binding free energy simulations. Int J Mol Sci. 2021 Aug 24;22(17):9124. doi: 10.3390/ijms22179124, PMID 34502033.
9. Eng H, Dantonio AL, Kadar EP, Obach RS, DI L, Lin J. Disposition of nirmatrelvir an orally bioavailable inhibitor of SARS-CoV-2 3C-like protease across animals and humans. Drug Metab Dispos. 2022 May;50(5):576-90. doi: 10.1124/dmd.121.000801, PMID 35153195.
10. Lam C, Patel P. Nirmatrelvir Ritonavir. In: Treasure Island (FL): StatPearls Publishing; 2024 Jan. Available from: https://www.ncbi.nlm.nih.gov/books/NBK585126. [Last accessed on 22 Nov 2024].
11. Marzi M, Vakil MK, Bahmanyar M, Zarenezhad E. Paxlovid: mechanism of action synthesis and in silico study. Bio Med Res Int. 2022 Jul 7;2022:7341493. doi: 10.1155/2022/7341493, PMID 35845944.
12. Katzenmaier S, Markert C, Riedel KD, Burhenne J, Haefeli WE, Mikus G. Determining the time course of CYP3A inhibition by potent reversible and irreversible CYP3A inhibitors using a limited sampling strategy. Clin Pharmacol Ther. 2011 Nov;90(5):666-73. doi: 10.1038/clpt.2011.164, PMID 21937987.
13. Anand K, Ziebuhr J, Wadhwani P, Mesters JR, Hilgenfeld R. Coronavirus main proteinase (3CLpro) structure: basis for design of anti-SARS drugs. Science. 2003 Jun 13;300(5626):1763-7. doi: 10.1126/science.1085658, PMID 12746549.
14. Marzolini C, Kuritzkes DR, Marra F, Boyle A, Gibbons S, Flexner C. Recommendations for the management of drug-drug interactions between the COVID-19 antiviral Nirmatrelvir/Ritonavir (Paxlovid) and comedications. Clin Pharmacol Ther. 2022 Dec;112(6):1191-200. doi: 10.1002/cpt.2646, PMID 35567754.
15. Chan GC, Lui GC, Wong CN, Yip SS, LI TC, Cheung CS. Safety profile and clinical and virological outcomes of nirmatrelvir ritonavir treatment in patients with advanced chronic kidney disease and coronavirus disease 2019. Clin Infect Dis. 2023 Nov 17;77(10):1406-12. doi: 10.1093/cid/ciad371, PMID 37531093.
16. Charness ME, Gupta K, Stack G, Strymish J, Adams E, Lindy DC. Rebound of SARS-CoV-2 infection after nirmatrelvir ritonavir treatment. N Engl J Med. 2022 Sep 15;387(11):1045-7. doi: 10.1056/NEJMc2206449, PMID 36069968.
17. Boucau J, Uddin R, Marino C, Regan J, Flynn JP, Choudhary MC. Characterization of virologic rebound following nirmatrelvir ritonavir treatment for coronavirus disease 2019 (COVID-19). Clin Infect Dis. 2023 Feb 8;76(3):e526-9. doi: 10.1093/cid/ciac512, PMID 35737946.
18. Anderson AS, Caubel P, Rusnak JM, EPIC-HR Trial Investigators. Nirmatrelvir-ritonavir and viral load rebound in COVID-19. N Engl J Med. 2022 Sep 15;387(11):1047-9. doi: 10.1056/NEJMc2205944, PMID 36069818.
19. Cho HY, Lee YB. Nano-sized drug delivery systems for lymphatic delivery. J Nanosci Nanotechnol. 2014 Jan;14(1):868-80. doi: 10.1166/jnn.2014.9122, PMID 24730304.
20. Hussain N, Jaitley V, Florence AT. Recent advances in the understanding of uptake of micro particulates across the gastrointestinal lymphatics. Adv Drug Deliv Rev. 2001 Aug 23;50(1-2):107-42. doi: 10.1016/s0169-409x(01)00152-1, PMID 11489336.
21. Pardeshi C, Rajput P, Belgamwar V, Tekade A, Patil G, Chaudhary K. Solid lipid-based nanocarriers: an overview. Acta Pharm. 2012 Dec;62(4):433-72. doi: 10.2478/v10007-012-0040-z, PMID 23333884.
22. Priyanka P, Sri Rekha M, Devi AS. Review on formulation and evaluation of solid lipid nanoparticles for vaginal application. Int J Pharm Pharm Sci. 2022 Jan;14(1):1-8. doi: 10.22159/ijpps.2022v14i1.42595.
23. Cai S, Yang Q, Bagby TR, Forrest ML. Lymphatic drug delivery using engineered liposomes and solid lipid nanoparticles. Adv Drug Deliv Rev. 2011 Sep 10;63(10-11):901-8. doi: 10.1016/j.addr.2011.05.017, PMID 21712055.
24. Mura P, Maestrelli F, D Ambrosio M, Luceri C, Cirri M. Evaluation and comparison of solid lipid nanoparticles (SLNs) and nanostructured lipid carriers (NLCs) as vectors to develop hydrochlorothiazide effective and safe pediatric oral liquid formulations. Pharmaceutics. 2021 Mar 24;13(4):437. doi: 10.3390/pharmaceutics13040437, PMID 33804945.
25. Gupta S, Kesarla R, Chotai N, Misra A, Omri A. Systematic approach for the formulation and optimization of solid lipid

nanoparticles of efavirenz by high-pressure homogenization using design of experiments for brain targeting and enhanced bioavailability. Bio Med Res Int. 2017;2017:5984014. doi: 10.1155/2017/5984014, PMID 28243600.
26. Ekambaram P, Abdul HS. Formulation and evaluation of solid lipid nanoparticles of ramipril. J Young Pharm. 2011 Jul;3(3):216-20. doi: 10.4103/0975-1483.83765, PMID 21897661.
27. Priyadarsini S, Lahoti SR. Quality by design: optimization of letrozole solid lipid nanoparticle for breast cancer. Ind J Pharm Edu Res. 2022;56(4):1013-24. doi: 10.5530/ijper.56.4.182.
28. Chokshi NV, Khatri HN, Patel MM. Formulation optimization and characterization of rifampicin-loaded solid lipid nanoparticles for the treatment of tuberculosis. Drug Dev Ind Pharm. 2018 Dec;44(12):1975-89. doi: 10.1080/03639045.2018.1506472, PMID 30058392.
29. Shah RM, Malherbe F, Eldridge D, Palombo EA, Harding IH. Physicochemical characterization of solid lipid nanoparticles (SLNs) prepared by a novel microemulsion technique. J Colloid Interface Sci. 2014 Aug 15;428:286-94. doi: 10.1016/j.jcis.2014.04.057, PMID 24910064.
30. Qushawy M, Nasr A, Abd Alhaseeb M, Swidan S. Design optimization and characterization of a transfersomal gel using miconazole nitrate for the treatment of candida skin infections. Pharmaceutics. 2018 Feb 23;10(1):26. doi: 10.3390/pharmaceutics10010026, PMID 29473897.
31. Kashanian S, Azandaryani AH, Derakhshandeh K. New surface modified solid lipid nanoparticles using N-glutaryl phosphatidylethanolamine as the outer shell. Int J Nanomedicine. 2011;6:2393-401. doi: 10.2147/IJN.S20849, PMID 22114489.
32. Singh S, Dobhal AK, Jain A, Pandit JK, Chakraborty S. Formulation and evaluation of solid lipid nanoparticles of a water-soluble drug: zidovudine. Chem Pharm Bull (Tokyo). 2010 May;58(5):650-5. doi: 10.1248/cpb.58.650, PMID 20460791.
33. Priyanka K, Sathali AA. Preparation and evaluation of montelukast sodium-loaded solid lipid nanoparticles. J Young Pharm. 2012 Jul;4(3):129-37. doi: 10.4103/0975-1483.100016, PMID 23112531.
34. Aslam R, Tiwari V, Upadhyay P, Tiwari A. Revolutionizing therapeutic delivery: diosgenin loaded solid lipid nanoparticles unleash advanced carriers. Int J App Pharm. 2024 Jan;16(1):124-33. doi: 10.22159/ijap.2024v16i1.49306.
35. Jain S, Mistry MA, Swarnakar NK. Enhanced dermal delivery of acyclovir using solid lipid nanoparticles. Drug Deliv Transl Res. 2011 Oct;1(5):395-406. doi: 10.1007/s13346-011-0036-0, PMID 25788423.
36. Shafique M, Khan MA, Khan WS, Maqsood-ur-Rehman, Ahmad W, Khan S. Fabrication characterization and *in vivo* evaluation of famotidine loaded solid lipid nanoparticles for boosting oral bioavailability. J Nanomater. 2017;2017:1-10. doi: 10.1155/2017/7357150.
37. Martens Lobenhoffer J, Boger CR, Kielstein J, Bode Boger SM. Simultaneous quantification of nirmatrelvir and ritonavir by LC-MS/MS in patients treated for COVID-19. J Chromatogr B Analyt Technol Biomed Life Sci. 2022 Dec 1;1212:123510. doi: 10.1016/j.jchromb.2022.123510, PMID 36274268.
38. Hassan H, Bello RO, Adam SK, Alias E, Meor Mohd Affandi MM, Shamsuddin AF. Acyclovir loaded solid lipid nanoparticles: optimization characterization and evaluation of its pharmacokinetic profile. Nanomaterials (Basel). 2020 Sep 9;10(9):1785. doi: 10.3390/nano10091785, PMID 32916823.
39. LI S, JI Z, Zou M, Nie X, Shi Y, Cheng G. Preparation characterization pharmacokinetics and tissue distribution of solid lipid nanoparticles loaded with tetrandrine. AAPS Pharm Sci Tech. 2011 Sep;12(3):1011-8. doi: 10.1208/s12249-011-9665-3, PMID 21811889.
40. Phalak SD, Bodke V, Yadav R, Pandav S, Ranaware M. A systematic review on nano drug delivery system: solid lipid nanoparticles (SLN). Int J Curr Pharm Sci. 2024 Jan;16(1):10-20. doi: 10.22159/ijcpr.2024v16i1.4020.
41. Aburahma MH, Badr Eldin SM. Compritol 888 ATO: a multifunctional lipid excipient in drug delivery systems and nanopharmaceuticals. Expert Opin Drug Deliv. 2014 Dec;11(12):1865-83. doi: 10.1517/17425247.2014.935335, PMID 25152197.
42. Gupta B, Sharma R. Formulation and *in vitro* characterization of the solid lipid nanoparticles of naftopidil for enhancing oral bioavailability. Asian J Pharm Clin Res. 2023;16(2):77-82. doi: 10.22159/ajpcr.2023.v16i2.46465.
43. Ekambaram P, Abdul HS. Formulation and evaluation of solid lipid nanoparticles of ramipril. J Young Pharm. 2011 Jul;3(3):216-20. doi: 10.4103/0975-1483.83765, PMID 21897661.
44. Chen WN, Shaikh MF, Bhuvanendran S, Date A, Ansari MT, Radhakrishnan AK. Poloxamer 188 (P188) a potential polymeric protective agent for central nervous system disorders: a systematic review. Curr Neuropharmacol. 2022;20(4):799-808. doi: 10.2174/1570159X19666210528155801, PMID 34077349.
45. Xia Y, FU S, MA Q, Liu Y, Zhang N. Application of nano delivery systems in lymph nodes for tumor immunotherapy. Nanomicro Lett. 2023;15(1):145. doi: 10.1007/s40820-023-01125-2, PMID 37269391.
46. Qushawy M, Prabahar K, Abd-Alhaseeb M, Swidan S, Nasr A. Preparation and evaluation of carbamazepine solid lipid nanoparticle for alleviating seizure activity in pentylenetetrazole kindled mice. Molecules. 2019 Nov 2;24(21):3971. doi: 10.3390/molecules24213971, PMID 31684021.
47. Gupta S, Kesarla R, Chotai N, Misra A, Omri A. Systematic approach for the formulation and optimization of solid lipid nanoparticles of efavirenz by high-pressure homogenization using design of experiments for brain targeting and enhanced bioavailability. Bio Med Res Int. 2017;2017:5984014. doi: 10.1155/2017/5984014, PMID 28243600.
48. Galli M, Migliano F, Fasano V, Silvani A, Passarella D, Citarella A. Nirmatrelvir: from discovery to modern and alternative synthetic approaches. Processes. 2024;12(6):1242. doi: 10.3390/pr12061242.
49. Remya PN, Damodharan N. Formulation development and characterization of cilnidipine loaded solid lipid nanoparticles. Asian J Pharm Clin Res. 2018;11(1):120-5. doi: 10.22159/ajpcr.2018.v11i9.24666.
50. Abdelbary G, Fahmy RH. Diazepam loaded solid lipid nanoparticles: design and characterization. AAPS Pharm Sci Tech. 2009;10(1):211-9. doi: 10.1208/s12249-009-9197-2, PMID 19277870.
51. Madgulkar AR, Padalkar RR, Amale SK. Preformulation studies of intranasal solid lipid nanoparticles of mometasone furoate. J Drug Delivery Ther. 2019;9(4):526-8. doi: 10.22270/jddt.v9i4.3100.
52. Shah J, Patel S, Bhairy S, Hirlekar R. Formulation optimization characterization and *in vitro* anti-cancer activity of curcumin loaded nanostructured lipid carriers. Int J Curr Pharm Sci. 2022 Jan;14(1):31-43. doi: 10.22159/ijcpr.2022v14i1.44110.
53. Paliwal R, Rai S, Vaidya B, Khatri K, Goyal AK, Mishra N. Effect of lipid core material on characteristics of solid lipid nanoparticles designed for oral lymphatic delivery. Nanomedicine. 2009;5(2):184-91. doi: 10.1016/j.nano.2008.08.003, PMID 19095502.
54. Hoshyar N, Gray S, Han H, Bao G. The effect of nanoparticle size on *in vivo* pharmacokinetics and cellular interaction. Nanomedicine (Lond). 2016 Mar;11(6):673-92. doi: 10.2217/nnm.16.5, PMID 27003448.
55. Chattopadhyay N, Zastre J, Wong HL, WU XY, Bendayan R. Solid lipid nanoparticles enhance the delivery of the HIV protease inhibitor atazanavir by a human brain endothelial cell line. Pharm Res. 2008 Oct;25(10):2262-71. doi: 10.1007/s11095-008-9615-2, PMID 18516666.